Received: 26 July 2022 | Revised: 23 November 2022 | Accepted: 3 December 2022

DOI: 10.1002/pc.27203

RESEARCH ARTICLE

Polymer COMPOSITES WILEY

Synthesis and characterization of sodium alginate/polyvinyl alcohol/zinc oxide/iron oxide nanocomposites for electrochemical applications

Hind Albalawi[1] | **Ebtesam M. Alharbi**[2] | **Ahlam I. Al-Sulami**[3] | **Noora Al-Qahtani**[4] | **Mohammed O. Farea**[5] | **A. Rajeh**[5]

[1]Department of Physics, College of Sciences, Princess Nourah Bint Abdulrahman University (PNU), Riyadh, Saudi Arabia

[2]Department of Physics, College of Science, University of Jeddah, Jeddah, Saudi Arabia

[3]Department of Chemistry, College of Science, University of Jeddah, Jeddah, Saudi Arabia

[4]Center for Advanced Materials (CAM), Qatar University, Doha, Qatar

[5]Physics Department, Faculty of Science, Mansoura University, Mansoura, Egypt

Correspondence
A. Rajeh, Physics Department, Faculty of Science, Mansoura University, Mansoura, Egypt.
Email: a.rajeh88@yahoo.com

Funding information
Princess Nourah Bint Abdulrahman University, Grant/Award Number: PNURSP2022R29

Abstract

Polymer nanocomposites films, based on sodium alginate (NaAlg) and polyvinyl alcohol (PVA) complexed with zinc oxide nanoparticles (ZnO NPs) and iron oxide nanorods (Fe_3O_4 NRs) as nanofiller, were prepared by solution casting technique. Different techniques were used to describe the prepared films. XRD and FTIR were used to pinpoint the complexation of the nanofiller with the polymer mixture. The XRD investigation verified the existence of the crystalline peaks of ZnO/Fe_3O_4 NPs in the polymeric matrices. The average particle size of nanocomposite was 23 nm. TEM image of the ZnO nanopowder confirming the spherical form of nanoparticles with average size 30 nm. The TEM image of Fe_3O_4 NRs reveals the free nanorods are around 9–23 nm in diameter and 130–350 nm in length. Peak positions and intensity variations in the FTIR absorption spectra are observed when the concentration increases from 2 to 8 wt% of ZnO NPs/Fe_3O_4 NRs. AC conductivity showed that the NaAlg/PVA-(8 wt%) ZnO/Fe_3O_4 NPs nanocomposites have higher electrical conductivity than NaAlg/PVA blend. For samples of 8% ZnO/Fe_3O_4, the σ_{dc} of nanocomposites reached 3.66×10^{-8} S cm^{-1}. ZnO/Fe_3O_4 nanoparticles considerably improved the nanocomposites' ability to conduct electricity. For the development of functional composite materials for the manufacture of electrical devices, sensors, and high-energy storage capacitors, the enhanced characteristics of synthesized NaAlg/PVA-ZnO/Fe_3O_4 nanocomposites can be helpful.

KEYWORDS

Ac conductivity, dielectric parameters, ZnO/Fe_3O_4 nanoparticles, ZnO/Fe_3O_4-NaAlg/PVA nanocomposites

1 | INTRODUCTION

Polymeric nanocomposites based on metal oxide nanoparticles have attracted a lot of attention recently due to their excellent chemical, electrical, and optical characteristics.[1–3] As a result, they are now used in a variety of products, including sensors, solar cells, batteries, fuel cells, and supercapacitors.[4–6] By combining polymers with metal oxide nanoparticles in the composite's structure, it is possible to improve the electrical characteristics of

certain polymers, such as conductivity and dielectric constant.[7] The hydrogen bonds that help to produce the polyvinyl alcohol (PVA)-based nanocomposites come from hydroxyl groups.[8] They are present in PVA, which has a significant capacity for holding charges and exhibits strong chemical, electrical, and dielectric properties. PVA has been widely used in a wide range of applications, including paper coating, textiles, packaging, electrochromic devices, artificial medical equipment, electrical devices, and membrane applications. Polymer blends provide a number of benefits, including being affordable and a novel way to create composites with improved chemical and physical characteristics for use in a variety of applications.[9,10]

Sodium alginate (NaAlg), an amorphous natural polymer that is biodegradable and nontoxic, is frequently used to help polyvinyl alcohol (PVA) establish its blend system by increasing the proportion of amorphous phases within PVA. Furthermore, adding NaAlg reduces the separation phase in the samples that have been produced.[8] The anionic nature of the NaAlg and its solubility in water are its distinguishing features. When hydroxyl groups are present, the NaAlg interacts with the additional polymers (such as PVA) through a hydrogen bond.[11,12] Sodium alginate is a suitable for use in several industries, including paper production, food packaging, pharmaceuticals, and electrical equipment due to its exceptional properties.[13,14] The distinctive features of nanoparticles and nanorods are closely connected to their size and distribution. Therefore, the production of Fe_3O_4 nanorods-supported nanomaterial is necessary because it possesses the properties of Fe_3O_4 nanorods and nanomaterial, making it beneficial in a variety of applications. Zinc oxide nanoparticles (ZnO NPs) have gained a great deal of attention due to their extraordinary chemical and optical features as well as their excellent electrical and catalytic abilities. The properties of ZnO NPs are mostly determined by their nonstructural characteristics, such as shape, crystal size and phase, aspect ratio, and distribution density.[15] The modification of Fe_3O_4 nanorods to achieve the desired shape, high dispersion, and improved size distribution of ZnO nanoparticles on the surface of the Fe_3O_4 nanorods results in the development of ZnO NPs/Fe_3O_4 NRs nanostructure.[16,17] Additionally, the sol–gel technique used to create ZnO NPs nanoparticles on the surface of Fe_3O_4 nanorods preserved their tiny particle size and narrow size distribution. With the addition of ZnO NPs/Fe_3O_4 NRs to the polymer mixture, the produced films surprisingly exhibit excellent characteristics. These characteristics are completely different from those of the conventional material.[18] The final product possesses excellent optical and electrical characteristics, allowing it to be applied in several domains like photo imaging, optics, sensor design, and so forth.[19] Shalumon et al.[20] created nanofibers by blended sodium alginate and polyvinyl alcohol. They stated that the obtained samples were appropriate for use in packaging, foods, cosmetic, and medicinal applications. Alghamdi and Rajeh studied the influences of titanium dioxide and carbon nanotubes on the optical, electrical, and mechanical characteristics of a PVA/NaAlg polymer composite. They found that the prepared samples exhibit excellent optical, dielectric constant, and mechanical characteristics, making them suitable for the fabrication of nanoelectronics devices with great energy storage capabilities.[21] The authors found no prior reports of the dielectric relaxation of a ZnO/Fe_3O_4 nanostructure doped with a polyvinyl alcohol (PVA) and sodium alginate (NaAlg) composition. As a result, the essential qualities of PVA/NaAlg and ZnO/Fe_3O_4 encouraged this study of PVA/NaAlg/ZnO/Fe_3O_4 nanocomposites films, which will focus on their physical, optical, electric, and dielectric characteristics with varied ZnO/Fe_3O_4 nanostructure ratios. The aim of this paper was to create zinc oxide/iron oxide nanoparticles in PVA/NaAlg samples using casting method to improve the physical properties of the PVA/NaAlg composite at different concentrations. The structural, morphological, electrical properties of the generated PVA/NaAlg/ZnO/Fe_3O_4 nanocomposites films were studied using XRD, TEM, FTIR, and AC.

2 | EXPERIMENTAL WORK

2.1 | Chemicals

PVA (polyvinyl alcohol) from E-Merck, Germany, having a molecular weight of 14,000 g/mol. NaAlg (sodium alginate) was purchased from National Research Centre Cairo with a M.W. of 3.5×10^5 g mol^{-1}. Zinc acetate dehydrate, $FeCl_3$, NaAc, oleic acid, and ethylene glycol were delivered by Sigma-Aldrich (Germany) with a purity of 99.996%. Double-distilled water (DDW) was used as a conventional solvent during sample preparation.

2.2 | ZnO nanoparticles synthesis

Chemical methods have been used to create zinc oxide nanoparticles. This process involves continuously swirling 0.2 M zinc acetate dihydrate ($(CH_3\text{-}COO)_2Zn{\cdot}2H_2O$) into di-methylene sulphoxide (DMSO). By using the same procedure, a 1.2 M potassium hydroxide (KOH) solution in ethanol has also been created. KOH solution has been added drop by drop after zincacetate has completely dissolved. Thioglycerol has been added, and the mixture has

been mixed. The precipitate has been eliminated and the solution has been centrifuged when it turns milky. As a result, ethanol was used to clean the precipitated ZnO nanoparticles before they were dried in the atmosphere.

2.3 | Preparation of Fe_3O_4 nanorods

The pre-synthesized Fe_3O_4 microspheres were placed in a three-necked flask with $FeCl_3$, $3H_2O$ (0.25 g), NaAc (1 g), oleic acid (25 ml), and ethylene glycol (25 ml) and stirred vigorously to form a black suspension. After obtaining the black suspension, a Teflon-lined autoclave with a capacity of 50 ml was used. We sealed the autoclave, heated it to 180°C for 8 h, and cooled it to room temperature. In the next step, centrifugation of the black precipitate was undertaken, subsequent washing in distilled water and absolute ethanol was performed, and finally drying at 60°C for 6 h under vacuum was performed.

2.4 | Synthesis of ZnO with Fe_3O_4 hybrids

ZnO/Fe_3O_4 hybrids were initially sonochemically synthesized by dispersing 0.2 g of functionalized ZnO in 20 ml of double-distilled water (DDW) for 2 h by means of ultrasonication. In addition, in a different beaker with a magnetic stirrer, 0.2 g of functionalized Fe_3O_4 were dissolved in 20 ml double-distilled water. The resulting two solutions were mixed and ultrasonically processed for 30 min at a power of 750 W, an amplitude of 20 kHz. Through this experiment, we obtained 40 ml of double-distilled water containing 0.4 g of ZnO and Fe_3O_4 with (50/50) ratio.

2.5 | Creation of PVA/NaAlg/-ZnO/Fe_3O_4 nanocomposite

PVA and NaAlg were each separately dissolved in double-distilled water to the desired concentration. The obtained solution is clear and transparent after 8 h. The PVA/NaAlg ratio of 70/30 was used in the casting process to create the polymer blend electrolytes. For 6 h, the synthesized ZnO/Fe_3O_4 was dispersed in double-distilled water to produce polymer nanocomposites with varying weight percentages (2, 4, 6, 8 wt%). Finally, all the solutions were combined and constantly agitated to create a viscous liquid of uniform consistency. The resulting solution was placed in a Petri dish. Polymer blend nanocomposites were created when the solvent gradually evaporated for 4 days. The PVA/NaAlg/-ZnO/Fe_3O_4 nanocomposites were peeled from the petri dish and utilized for further analysis.

2.6 | Physical examination

The X-ray diffraction spectra of polymer nanocomposite samples with various percentages of ZnO/Fe_3O_4 were studied using a Diano XRD 800 diffractometer (DIANO Corporation, Woburn, MA) with a Ni filter and Cu K_α radiation of $\lambda = 1.5406$. FT-IR spectroscopy (Nicolet iS10, USA) with a resolution of 3 cm^{-1} is used to determine the functional groups in the current polymer matrices. The size and form of ZnO/Fe_3O_4 were examined using a transmission electron microscope (JEOL 1200 EX apparatus at $V = 120$ kV Japans). The UV–Vis spectra for films formed of polymer nanocomposites were acquired at room temperature using a JASCO UV–VIS Spectrometer (Model V-630, Japan) automated recording double beam spectrophotometer. Broadband dielectric spectroscopy (Novocontrol Turnkey Concept 40 System; Novocontrol Technologies) has been used to analyze impedance from 0.1 Hz to 20 MHz in a dry nitrogen atmosphere.

3 | RESULTS AND DISCUSSION

3.1 | XRD and TEM

The XRD pattern of prepared ZnO NPs is shown in Figure 1A. ZnO NPs reflection peaks were observed at 2θ values 31.74°, 33.92°, 36.24°, 47.22°, 56.71°, 62.71°, 67.57°, and 69.08° are indexed to hexagonal phase of ZnO nanoparticles (COD ID: 2300450).[22] Debye–Scherrer Equation has been used to calculate the average particle size[23] which comes out as 23 nm. Figure 1B shows typical TEM micrograph of the ZnO nanopowder confirming the spherical form. The estimated average size of the nanoparticle is 30 nm, which is in good agreement with size estimates in XRD data. A typical XRD pattern of Fe_3O_4 prepared at 180°C under solvothermal conditions is shown in Figure 1C. The pattern showed peaks at 28.72°, 34.38°, 41.78°, 55.91°, and 61.57° which can be attributed to Fe_3O_4 (JCPDS no. 19-629). By utilizing these Fe_3O_4 microspheres as growth substrates, it was possible to produce Fe_3O_4 nanorods on the microspheres' surfaces. The findings of the experiments show that the nanorods are only lightly connected to the surfaces of the microspheres, and that ultrasonic treatment might be used to collect them. The TEM image in Figure 1D reveals that the free nanorods are around 9–23 nm in diameter and 130–350 nm in length.

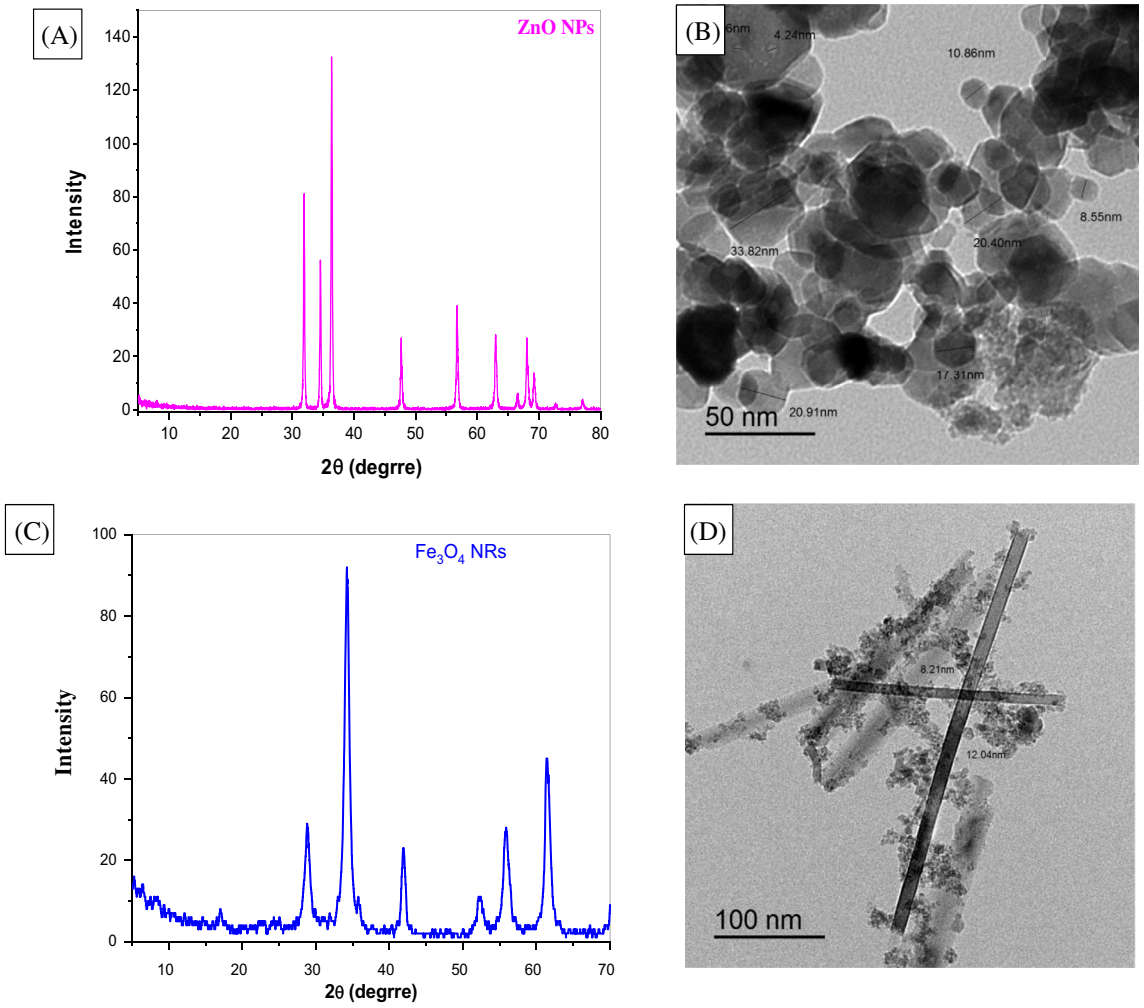

FIGURE 1 (A) XRD pattern of pure ZnO NPs and (B) TEM image of ZnO NPs. (C) XRD pattern of pure Fe_3O_4 NRs and (D) TEM image of Fe_3O_4 NRs

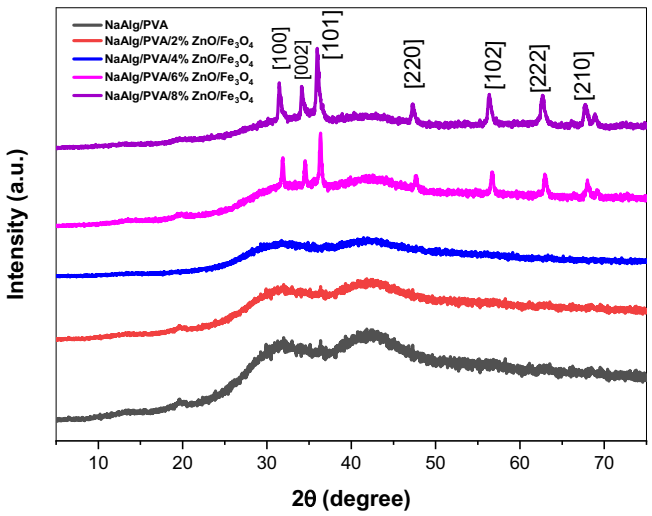

FIGURE 2 XRD pattern of PVA/NaAlg and PVA/NaAlg with various concentrations of ZnO/Fe_3O_4 NPs

To determine the effect of ZnO/Fe_3O_4 NPs on the pure NaAlg/PVA polymer structure and NaAlg/PVA-ZnO/Fe_3O_4 nanocomposites samples, XRD examinations were conducted, as shown in Figure 2. For pure NaAlg/PVA blend, a broad peak occurred in the 2θ (25.8–42.7), confirming its amorphicity due to its irregular structure.[24] This broad reveals the amorphous nature of the complex system, and the findings can be explained in terms of Hodge et al.[25] who discovered a connection between peak intensity and crystallinity level. We found that the intensity of the XRD pattern decreased as the material's amorphousness increased as a result of the dopant addition. This improves the conductivity properties of the NaAlg/PVA mixture and enables the considerable mobility of polymer chains in the amorphous phase. All peaks of ZnO/Fe_3O_4 NPs disappeared in nanocomposites at contents ≤4 wt% due to the fine dispersion of ZnO/Fe_3O_4 NPs in amorphous regions of the blend.[26]

TABLE 1 XRD study of the PVA/NaAlg characteristic peak

Sample	Characteristic peak	Crystallinity (%)	D (nm)	ε	δ, $\times 10^{16}$ (m^{-2})
PVA/NaAlg	-	45.23	-	-	-
PVA/NaAlg/2% (ZnO/Fe_3O_4)	-	37.76	-	-	-
PVA/NaAlg/4% (ZnO/Fe_3O_4)	-	32.64	-	-	-
PVA/NaAlg/6% (ZnO/Fe_3O_4)	36.24	27.82	4.32	0.0459	5.3
PVA/NaAlg/8% (ZnO/Fe_3O_4)	36.24°	18.42	3.89	0.0359	6.6

But at contents ≥6 wt%, it is noticed that the diffraction peaks at 2θ = 31.74°, 34.38°, 36.24°, 47.22°, 56.71°, 62.71°, 67.57°, and 69.08° that appeared are assigned to ZnO/Fe_3O_4 NPs, which increase (intensity) with increasing ZnO/Fe_3O_4 NPs content in the nanocomposites films. At low concentrations, these new peaks are more prominent broad, and less intense (6%), which gradually gets less broad and more intense. This shows that the particles in the NaAlg/PVA matrix are growing. The NaAlg/PVA matrix's growing filler content causes particle agglomeration, which is the cause of this growth. Additionally, this might be connected to the connections created between the functional groups of the NaAlg/PVA and the nanofiller as well as the intermolecular interactions. More polymer structural disorder results from this, which has an impact on the matrix's packing density. Hermans and Weidinger method is used to calculate the crystallinity (X_c).[27]

$$\text{Crystallinity}\,(X_c) = (A_c/A_T) \times 100. \quad (1)$$

In this method, A_c is area of amorphous haloes and A_T is the total area of peaks (area of amorphous and crystalline peak). As shown in Table 1, the crystallinity was observed to reduce from 45.23 for pure NaAlg/PVA to about 18.42 for NaAlg/PVA film doped with 8% ZnO/Fe_3O_4 NPs. In addition, the doping of ZnO/Fe_3O_4 NPs affected on the microstrain (ε), dislocation density (δ) and the particle size (D), of pure NaAlg/PVA and the nanocomposites samples. The following equations can be used to determine these parameters.[28,29]

$$D = 0.9\lambda/\beta \cos\theta, \quad (2)$$

$$\varepsilon = \beta/4 \tan\theta, \quad (3)$$

$$\delta = 1/D^2, \quad (4)$$

where, β is the typical peak's full width at half maximum (FWHM) and λ is the wavelength of Cukα-radiation. On the basis of the characteristic peak (1 0 1) of NaAlg/PVA samples, the D, ε, and δ values are computed. The results tabulated in Table 1.

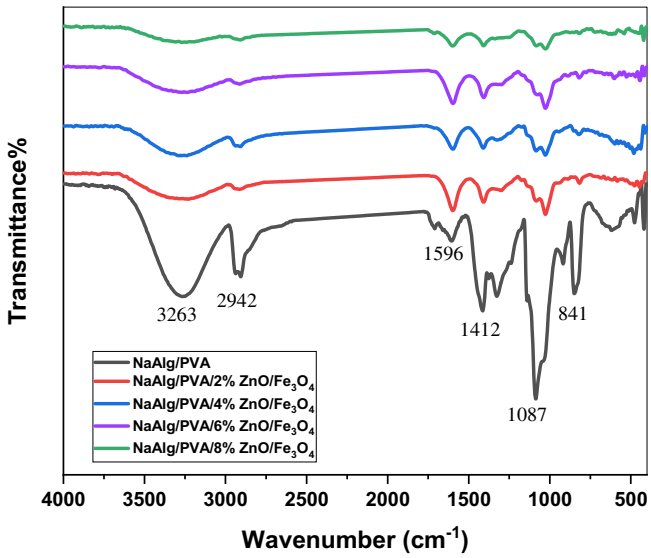

FIGURE 3 FT-IR transmittance bands of PVA/NaAlg blend and PVA/NaAlg filled with different concentrations of ZnO/Fe_3O_4 nanoparticles/nanorods

3.2 | FT-IR bands

The FT-IR transmittance bands of the PVA/NaAlg polymer blend and PVA/NaAlg-ZnO/Fe_3O_4 nanocomposite is shown in Figure 3. The prominent FT-IR transmittance bands of PVA/NaAlg are ascribed to the hydroxyl (OH) stretch at 3263 cm^{-1}, asymmetric and symmetric CH_2 stretch at 2942 and 2909 cm^{-1}, respectively, CH_2 wagging at 1412 cm^{-1} and OH bending at 1332 cm^{-1}, and C—O stretch from crystallinity at 1148 cm^{-1}. The band at 1087 cm^{-1} relates to C═O stretch and OH bending; the band at 921 cm^{-1} refers to CH_2 bending and the band at 841 cm^{-1} corresponds to CH rocking.[30] In the presence of ZnO/Fe_3O_4, the O—H and C—H groups may have induced out-of-plane vibrations that resulted in the weakening of PVA/NaAlg and a decrease in the FT-IR

SCHEME 1 (a, b) Possible interactions with the PVA/NaAlg/ZnO NPs/Fe_3O_4 NRs nanocomposites

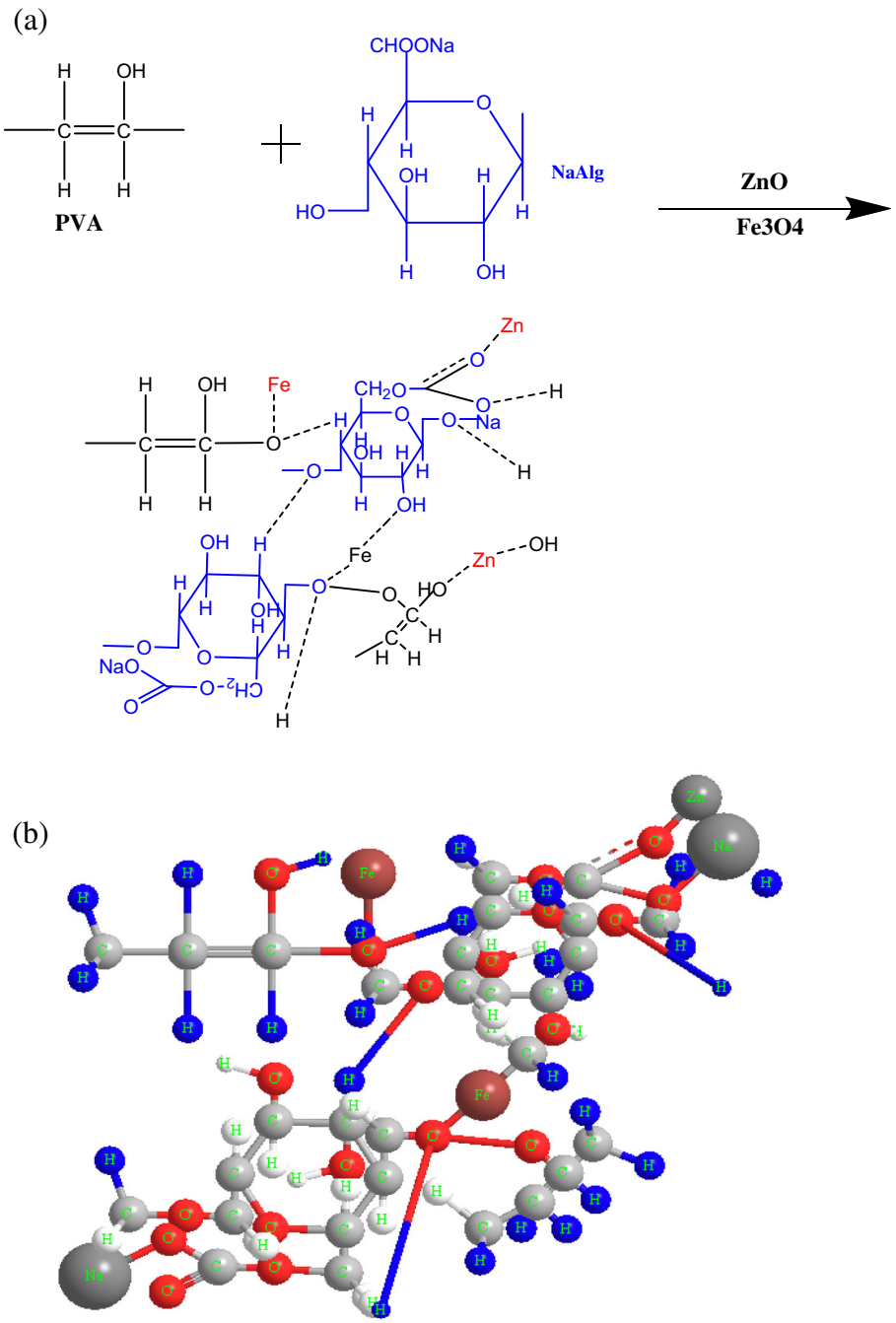

transmittance bands at 611 and 841 cm^{-1}, respectively. The vibration at 1087 cm^{-1} decreased and shifted to a lower wavenumber due to the interaction between the C═O group and metal ions. A decrease in the crystallinity of PVA/NaAlg was also indicated by a reduction in the intensity of the 1148 cm^{-1} band.[31] Reduction in the intensities of the bands at 1332 and 1412 cm^{-1}, showing decoupling between OH and CH vibrations, were confirmed by the weak contact between ZnO/Fe_3O_4 and PVA/NaAlg[32] (Scheme 1). The presence of most transmittance band of PVA and NaAlg in the polymer blend curve will confirms the miscibility and compatibility between two pure polymers. Characteristic bands at 3265 cm^{-1} (OH stretch) and 2923 cm^{-1} (C—H stretch) were present in the FT-IR transmittance bands of NaAlg. The symmetric and asymmetric stretching vibrations of C═O were ascribed to the bands at 1606 and 1403 cm^{-1}, respectively, and the C—C—H and O—C—H, C—O, and C—O—C stretching vibrations of pyranose rings were responsible for the bands at 1251, 1053, and 963 cm^{-1}, respectively. Metal ion interactions caused the NaAlg transmittance bands at 1406 cm^{-1} to shift to a lower wavenumber.[33] However, FT-IR spectra of ZnO/Fe_3O_4-containing polymeric nanocomposites did not reveal any appreciable

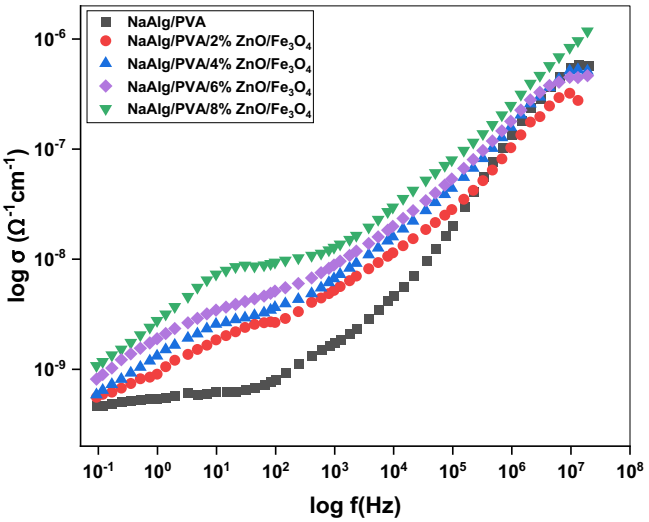

FIGURE 4 Logarithm of frequency (log f) versus logarithm of conductivity (log σ) of PVA/NaAlg blend, and PVA/NaAlg doped with different concentrations of ZnO NPs/Fe_3O_4NRs

metal-to-alginate bonding interactions, indicating that ZnO/Fe_3O_4 interacted with the alginate matrix primarily through van der Waals forces. PVA and NaAlg interacted in the PVA/NaAlg/ZnO/Fe_3O_4 nanocomposite as evidenced by changes in the intensity and shift of their FT-IR transmittance bands when they were present in different polymeric nanocomposites as in Scheme 1.[34]

3.3 | Electrical measurements

Figure 4 shows the relationship between the logarithm of frequency (log f) and the logarithm of conductivity (log σ) of a polymeric mixture (PVA/NaAlg) doped with various concentrations of ZnO NPs/Fe_3O_4 NRs. As the concentration of the nanofiller was increased, the conductivity of the current samples improved. In the low-frequency domain, there was a dispersion caused by spatial charge or interpolarization.[35] There were less mobile ions associated with charged particles at film surfaces, which contributed to the loss in conductivity at lower frequencies.[36] An increase in the amount of dopants led to an enhancement in electrical conductivity because the nanocomposites molecules start to reduce the potential barriers separating two localized states, bridging the gap between them, and facilitating charge carrier movement.[37] This enhancement was also attributed to the high conductivity of the extra NPs and the elevated charge mobility resulting from the expanded amorphous regions inside the doped films. The Jonscher power formula was used to determine the values of conductivity.

TABLE 2 The σ_{dc} and s values for the nanocomposite's samples

Samples	σ_{dc} (S cm^{-1})	s
PVA/NaAlg	1.85×10^{-9}	0.71
PVA/NaAlg/with 2% (ZnO/Fe_3O_4)	2.12×10^{-9}	0.63
PVA/NaAlg/with 4% (ZnO/Fe_3O_4)	2.58×10^{-8}	0.57
PVA/NaAlg/with 6% (ZnO/Fe_3O_4)	3.42×10^{-8}	0.52
PVA/NaAlg/with 8% (ZnO/Fe_3O_4)	3.66×10^{-8}	0.49

$$\sigma(\omega) = \sigma_{dc} + A\omega^{s}, \tag{5}$$

where, s refers to the exponent factor, means the angular frequency, and σ_{dc} indicates for electrical conductivity. The obtained values for σ_{dc} and s are shown in Table 2. Since the resultant values of s were substantially less than 1, it was concluded that these materials utilized a hopping mechanism for charge conduction.[38] For samples of 8% ZnO/Fe_3O_4, the σ_{dc} of nanocomposites reached 3.66×10^{-8} S cm^{-1}. A three-dimensional conductive channel was also formed by the NPs within the polymeric nanocomposite films, as seen by the increases in dc values.[37] Based on the dc results, we conclude that these polymer nanocomposite films can be considered for use in microelectronic devices as flexible polymeric nanodielectrics and the development of novel nanocomposite.

3.4 | Dielectric parameters

The dielectric constant and dielectric loss of a polymer composite and a blend filled with varying amounts of ZnO NPs/Fe_3O_4NRs were measured at room temperature across the frequency range of 10 Hz to 20 MHz. The dielectric characteristics' values were determined using the following relationships[39]:

$$\varepsilon' = \frac{Cd}{\varepsilon_0 A}, \tag{6}$$

$$\varepsilon'' = \frac{\sigma}{\omega\varepsilon_0}, \tag{7}$$

where, ε' represented the real part and ε'' represented the imaginary part, ε_0 denoted the permittivity of free space and C denoted the capacitance of the sample under investigation. The spectra of ε' and ε'' against log frequency of PVA/NaAlg polymer blend and PVA/NaAlg filled with various quantities of ZnO NPs/Fe_3O_4 NRs were shown in Figures 5 and 6. The resultant samples' spectra were shown to reduce nonlinearly with increasing frequency while enhancing with different nanofiller concentrations.

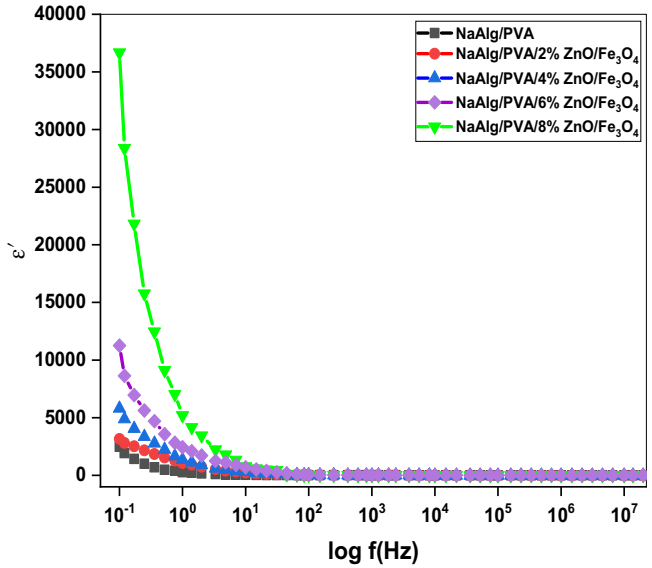

FIGURE 5 Logarithm of frequency (log f) versus ε' of PVA/NaAlg blend, and PVA/NaAlg doped with different concentrations of ZnO NPs/Fe_3O_4NRs

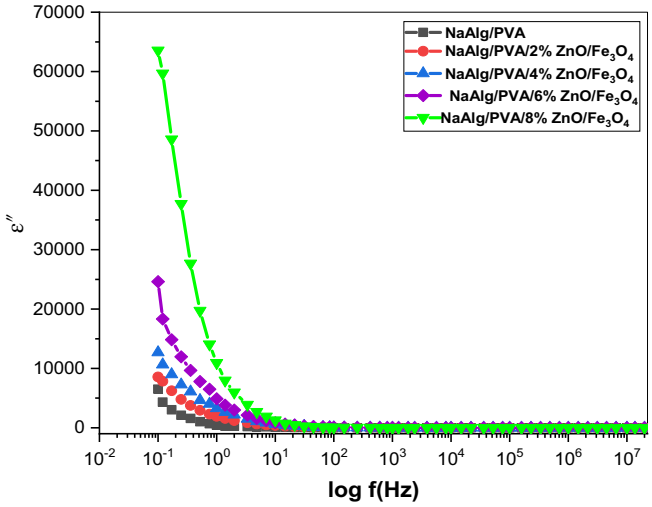

FIGURE 6 Logarithm of frequency (log f) versus ε'' of PVA/NaAlg blend, and PVA/NaAlg doped with different concentrations of ZnO NPs/Fe_3O_4NRs

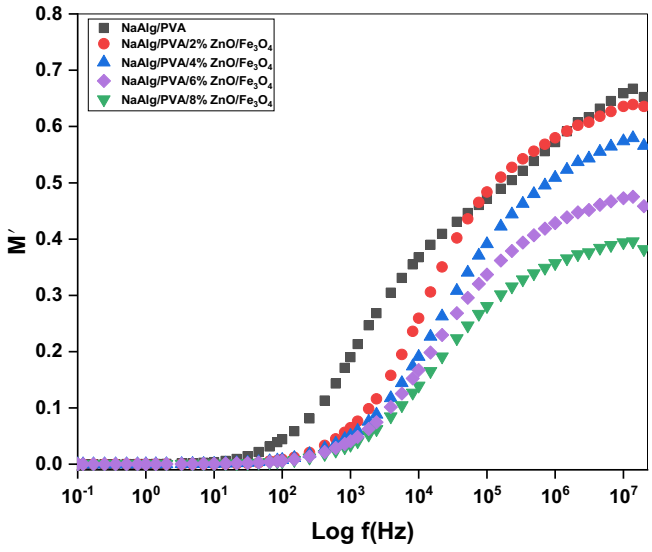

FIGURE 7 Logarithm of frequency (log f) versus M' of PVA/NaAlg blend, and PVA/NaAlg doped with different concentrations of ZnO NPs/Fe_3O_4NRs

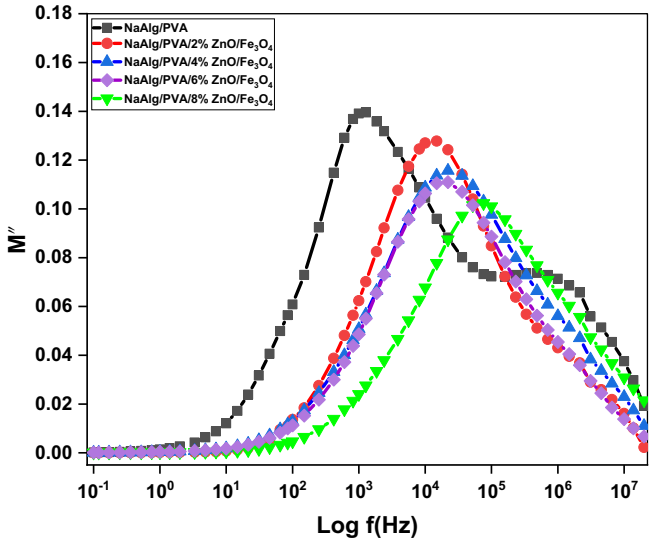

FIGURE 8 Logarithm of frequency (log f) versus M'' of PVA/NaAlg blend, and PVA/NaAlg doped with different concentrations of ZnO NPs/Fe_3O_4 NRs

The dielectric spectra of these nanocomposite samples significantly decreased with frequency due to the presence of interfacial polarization at the interfaces of various conductivity elements. The fact that dipoles in polymer films have a propensity to align in the direction of the applied field also contributed to the high value of the real and imaginary parts of the dielectric in the low frequency region. At high frequencies, the complex permittivity is essentially frequency-independent. There is no further ion propagation in the direction of the applied field because the periodic reversal of the electrical field at high frequencies happens so fast. The values of ε' and ε'' decreased as a result of the charge accumulation, which also caused a lower in polarization. After the addition of zinc and iron oxide, there were more parallel aligned dipoles in the PVA/NaAlg composite, which was represented in an increase in the real and imaginary parts of the dielectric constant at lower frequencies and a roughly equal increment at higher frequencies.[40]

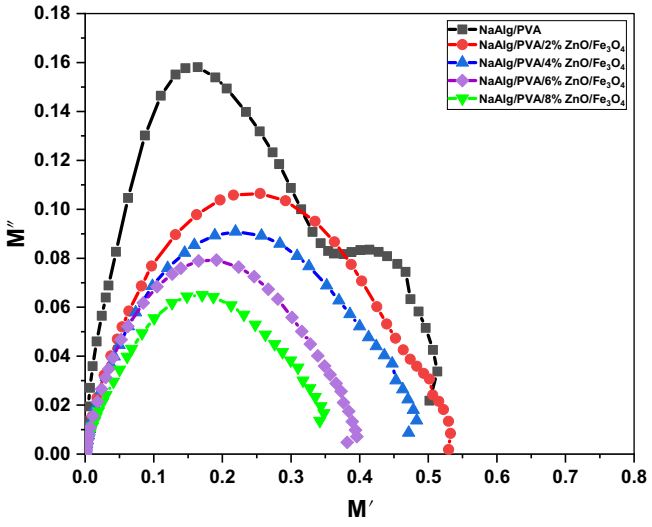

FIGURE 9 Variation of M'' versus M' of PVA/NaAlg blend, and PVA/NaAlg doped with different concentrations of ZnO NPs/Fe_3O_4 NRs

3.5 | Electric modulus

Electric modulus analysis was performed on the obtained samples to remove any potential influences from the electrode material, electrode polarization, or contact between the dielectric and electrodes. The real component (M') and imaginary part (M'') of the complex electric modulus spectra were calculated using the following equations[41]:

$$M' = \frac{\varepsilon'}{\varepsilon'^2 + \varepsilon''^2}, \tag{8}$$

$$M'' = \frac{\varepsilon''}{\varepsilon'^2 + \varepsilon''^2}. \tag{9}$$

The M' and M'' spectra of the produced samples and nanocomposite films at room temperature are depicted in Figures 7 and 8, respectively. At low frequencies, the eradication of electrode polarization was indicated by basically negative M' values, whereas the M' values of obtained samples increased nonlinearly with frequency. The Maxwell-Wagner-Sillars (MWS) process explains the mid-frequency relaxation in the M'' spectra of the generated films.[40] The relaxation peak of the doped films was shifted toward higher frequencies when compared to the PVA/NaAlg matrix, demonstrating that interactions between the polymer and nanofiller reduced impediment to the relaxation process and the relaxation period decreased as the nanofiller concentration increased. Conductivity relaxation dynamic is shown as a half-circle Argand plot (M'' vs. M') in Figure 9 for the nanocomposites samples, confirming the absence of contact effects and a Debye-type relaxation process (pure ionic relaxation).[42] The diameter of semicircles decreased as the concentration of ZnO/-Fe_3O_4 increase, as seen by the plots of nanocomposites samples, which is supported by the results. This is because there was less resistance to charge flow and more ionic mobility.

4 | CONCLUSION

The casting process made it simple to create flexible nanocomposites films made of ZnO/Fe_3O_4 and a combination of NaAlg/PVA polymer. These films were then thoroughly analyzed using different spectroscopic techniques. Successful manufacturing of NaAlg/PVA/ZnO/Fe_3O_4 nanocomposites films is demonstrated by the XRD and FTIR. XRD results demonstrate that the crystallite size of ZnO/Fe_3O_4 NPs rises with increasing the concentration of ZnO/Fe_3O_4 inside NaAlg/PVA blend. According to the FTIR absorption spectra, the peak positions changed with decreasing frequency, as well as transmission values fluctuated due to the different concentrations of ZnO NPs and Fe_3O_4 NRs. Increasing the amount of ZnO/Fe_3O_4 NPs in the polymeric matrix has also improved Ac's electrical conductivity and dielectric characteristics. In addition, as the concentration of nanofiller increases, the electric modulus, and complex impedance decline. The NaAlg/PVA/ZnO/Fe_3O_4 flexible nanocomposites films could be used in batteries, supercapacitors, and high-charge storage capacitive applications in microelectronic devices thanks to the advances that were described in this study.

ACKNOWLEDGMENT

This research was funded by the Princess Nourah Bint Abdulrahman University Researchers Supporting Project number (PNURSP2022R29), Princess Nourah Bint Abdulrahman University, Riyadh, Saudi Arabia.

CONFLICT OF INTEREST

The authors declare that they have no known competing financial interests or personal relationships that could have appeared to influence the work reported in this paper.

DATA AVAILABILITY STATEMENT

The data that support the findings of this study shall be made available from the corresponding author upon reasonable request.

ORCID

A. Rajeh https://orcid.org/0000-0002-5789-0599

REFERENCES

[1] M. J. Mochane, J. Sefadi, T. Motsoeneng, T. Mokoena, T. Mofokeng, M. Teboho, *Polym. Compos.* **2020**, *41*(7), 2958.
[2] M. A. Nunes, B. Matos, G. Silva, E. Ito, T. Jeferson, G. J. M. Fechine, *Polym. Compos.* **2021**, *42*(2), 661.
[3] L. Gautam, S. G. Warkar, S. I. Ahmad, R. Kant, M. Jain, *Polym. Eng. Sci.* **2022**, *62*, 225.
[4] E. Sharifzadeh, Y. J. P. C. Amiri, *Polym. Compos.* **2020**, *41*(9), 3585.
[5] C. M. Sai Prasanna, S. J. P. C. Austin Suthanthiraraj, *Polym. Compos.* **2019**, *40*(9), 3402.
[6] O. A. Alo, I. O. Otunniyi, H. J. P. C. Pienaar, *Polym. Compos.* **2020**, *41*(8), 3364.
[7] C. Zhang, Q. Chi, J. Dong, Y. Cui, X. Wang, L. Liu, Q. Lei, *Sci. Rep.* **2016**, *6*(1), 1.
[8] M. Farea, A. Abdelghany, A. J. R. A. Oraby, *RSC Adv.* **2020**, *10*(62), 37621.
[9] M. Mohanapriya, K. Deshmukh, K. Chidambaram, M. Basheer Ahamed, K. K. Sadasivuni, D. Ponnamma, M. Al-Ali AlMaadeed, R. R. Deshmukh, S. K. Khadheer Pasha, *J. Mater. Sci.: Mater. Electron.* **2017**, *28*(8), 6099.
[10] S. Sit, K. Nath, N. Das, G. Chakraborty, *Polym. Compos.* **2022**, *54*(6), 975.
[11] V. Hebbar, R. Bhajantri, J. Naik, *J. Mater. Sci.: Mater. Electron.* **2017**, *28*(8), 5827.
[12] N. Rajeswari, S. Selvasekarapandian, S. Karthikeyan, C. Sanjeeviraja, Y. Iwai, J. Kawamura, *Ionics* **2013**, *19*(8), 1105.
[13] M. Farea, R. Pashameah, K. Sharma, E. Alzahrani, A. Al-Muntaser, M. Sugair, M. Morsi, *Polym. Bull.* **2022**, 1. https://doi.org/10.1007/s00289-022-04498-3
[14] K. Suhailath, M. T. Ramesan, *J. Vinyl Addit. Technol.* **2019**, *25*, 9.
[15] S. Agarwal, V. K. Saraswat, *Opt. Mater.* **2015**, *42*, 335.
[16] R. Hong, S. Zhang, G. Di, H. Li, Y. Zheng, J. Ding, D. Wei, *Mater. Res. Bull.* **2008**, *43*(8–9), 2457.
[17] J. Xia, A. Wang, X. Liu, Z. Su, *Appl. Surf. Sci.* **2011**, *257*(23), 9724.
[18] A. R. Polu, R. Kumar, *Int. J. Polym. Mater.* **2013**, *62*(2), 76.
[19] L. Tamayo, H. Palza, J. Bejarano, P. A. Zapata, *Polymer Composites with Functionalized Nanoparticles*, Elsevier, **2019**, p. 249. 10.1016/B978-0-12-814064-2.00008-1
[20] K. Shalumon, A. Haridas, S. Nair, K. P. Chennazhi, R. Jayakumar, *Int. J. Biol. Macromol.* **2011**, *49*(3), 247.
[21] L. M. Al-Harbi, Q. Alsulami, O. M. Farea, A. Rajeh, *J. Mol. Struct.* **2023**, *1272*, 134244.
[22] T. Soliman, M. Hessien, S. I. Elkalashy, *J. Non-Cryst. Solids* **2022**, *580*, 121405.
[23] M. Abutalib, A. Rajeh, *Polym. Test.* **2020**, *91*, 106803.
[24] M. R. Atta, N. Algethami, M. O. Farea, Q. A. Alsulami, A. Rajeh, *Int. J. Energy Res.* **2022**, *46*(6), 8020.
[25] R. Hodge, G. H. Edward, G. P. Simon, *Polymer* **1996**, *37*(8), 1371.
[26] M. Abutalib, A. Rajeh, *Polym. Test.* **2021**, *93*, 107013.
[27] M. Abutalib, A. Rajeh, *J. Organomet. Chem.* **2020**, *920*, 121348.
[28] H. M. Alghamdi, A. Rajeh, *Int. J. Energy Res.* **2022**, *46*(14), 20050.
[29] I. Morad, A. M. Alshehri, A. F. Mansour, M. H. Wasfy, M. M. el-Desoky, *Phys. B* **2020**, *597*, 412415.
[30] M. A. Morsi, E. Abdelrazek, R. M. Ramadan, I. Elashmawi, A. Rajeh, *Polym. Test.* **2022**, *114*, 107705.
[31] M. Atta, E. O. Taha, A. Abdelreheem, *Appl. Phys. A* **2021**, *127*(7), 1.
[32] T. Vodnik, G. Kaljevic, T. Tadic, N. Majkic-Singh, *Clin. Chem. Lab. Med. (CCLM)* **2013**, *51*(10), 2053.
[33] R. Sharma, S. Patel, K. Pargaien, *Adv. Nat. Sci.: Nanosci. Nanotechnol.* **2012**, *3*(3), 035005.
[34] W.-B. Zeng, H. F. Jiang, Y. D. Gang, Y. G. Song, Z. Z. Shen, H. Yang, X. Dong, Y. L. Tian, R. J. Ni, Y. Liu, N. Tang, X. Li, X. Jiang, D. Gao, M. Androulakis, X. B. He, H. M. Xia, Y. Z. Ming, Y. Lu, J. N. Zhou, C. Zhang, X. S. Xia, Y. Shu, S. Q. Zeng, F. Xu, F. Zhao, M. H. Luo, *Mol. Neurodegen.* **2017**, *12*(1), 1.
[35] D. A. Nasrallah, M. A. Ibrahim, *J. Polym. Res.* **2022**, *29*(3), 1.
[36] M. Morsi, S. A. El-Khodary, A. Rajeh, *Phys. B* **2018**, *539*, 88.
[37] R. J. Sengwa, S. Choudhary, P. Dhatarwal, *J. Mater. Sci.: Mater. Electron.* **2019**, *30*(13), 12275.
[38] E. M. Alharbi, A. Rajeh, *J. Mater. Sci.: Mater. Electron.* **2022**, *33*(28), 22196.
[39] A. Abdelghany, M. Farea, A. Oraby, *J. Mater. Sci.: Mater. Electron.* **2021**, *32*(5), 6538.
[40] H. S. Alzahrani, A. I. Al-Sulami, Q. A. Alsulami, A. Rajeh, *Opt. Mater.* **2022**, *133*, 112900.
[41] A. Abdelghany, A. Oraby, M. Farea, *Phys. B* **2019**, *560*, 162.
[42] A. Rajeh, M. Morsi, I. Elashmawi, *Vacuum* **2019**, *159*, 430.

How to cite this article: H. Albalawi, E. M. Alharbi, A. I. Al-Sulami, N. Al-Qahtani, M. O. Farea, A. Rajeh, *Polym. Compos.* **2023**, *44*(3), 1762. https://doi.org/10.1002/pc.27203